

THE EFFECT OF MOISTURE AND STRUCTURE ON WET WEB STRENGTH AND ITS VARIATION – A PILOT SCALE APPROACH USING DRY AND REWETTED MILL MADE PAPERS

Markku Ora¹ and Thaddeus Maloney²

¹ UPM-Kymmene Corporation, Research Centre, FI-53200 Lappeenranta,
Finland

² School of Chemical Technology, Aalto University, FI-00076 Espoo, Finland

ABSTRACT

In spite of extensive research on wet web strength properties and rheology, knowledge of the effect of web structure, e.g. formation and fibre orientation, on wet web strength properties has been limited. Therefore the topic was studied by running the re-wetted mill-made paper reels on a pilot runnability device at low dry solids contents of 56% and 68%. In addition, one trial was conducted by measuring the wet web strength properties in situ on the press section of a pilot Fourdrinier. The benefit of both these approaches is the ability to measure the strength properties in more realistic conditions compared with standard laboratory methods.

In order to differentiate between the effect of formation and fibre orientation on strength properties, the variables should not be correlated. This requirement was met in the main mill trial by suitably selecting the headbox and wire section parameters. Formation was measured using a β -radiographic method and local grammage

variation was examined as standard deviation in different wavelength bands and size classes. In addition, formation was also measured with Ambertec formation tester. Fibre orientation was determined using layered fibre orientation measurements.

It was shown that formation has an influence on the tensile strength variation and the effect depends on the scale of formation and dry solids content. In contrast to dry strength, the wet strength does not follow the Weibull distribution, but rather the Gaussian one. In addition, the distribution of wet strength is sensitive to centimetre-scale variability in paper structure instead of millimetre-scale in dry paper. When formation is good, as it typically is on modern paper machines, further improvement does not improve average wet strength properties. Only when large scale formation is poor, it has an influence on average wet web tensile strength and tensile stiffness. Presumably this would be the situation on a Fourdrinier type machine. Unlike formation, anisotropy does not affect the strength variation but it has an influence on the average tensile strength and tensile stiffness of wet and dry papers. The anisotropy profile in z-direction has no influence on the mentioned properties.

1 INTRODUCTION

Paper machine runnability is a topic of intense interest to papermakers. Much research has been carried out concerning wet web rheology, wet web behaviour in an open draw and in the drying section, the effect of furnish and chemistry-related issues on wet web strength properties, bonding mechanism and the rupture mechanism. However, very little attention has been paid to the effect of web structure on wet web strength properties. Certainly, there are publications where the topic has been approached with modelling [1–5], but due to computational restrictions the size of the simulated specimens have been too small to allow study of the effects of formation scale grammage variation. In addition, there are published exercises [6, 7] using finite element simulations and experimental analysis. In addition to these publications, there are results available concerning the effect of fibre orientation on the tensile strength of the wet web [8].

However, the current knowledge related to the effect of paper structure on wet web strength properties is limited. For example, what is the effect of formation on wet web strength properties? Also it is unknown whether the strength of wet paper follows any extreme value distribution at all—as dry paper does.

This paper aims at answering these questions based on pilot scale measurements using mill made rewetted paper reels and in situ measurements on a pilot paper machine.

1.1 Bonding mechanism in wet webs

Campbell [9] suggested that wet paper is held together by capillary forces arising from an attractive capillary pressure in liquid bridges between fibres. Page [10] extended this idea and presented that the wet web tensile strength can be considered in terms of the frictional shear strength of the fibre-fibre crossings that are pulled into contact by the surface tension forces in the water menisci. Shallhorn [11] modified Page's theory by taking into account the effect of wet pressing on fibre thickness and relative bonded area. His results suggest that surface tension forces are responsible for wet web tensile properties over a wide range of moisture contents corresponding to dry solids contents ~ 20–60%. The model he used is limited to the fibre fraction of softwood kraft. As such, no fines were involved. In any case, there was good agreement between the predicted and measured tensile strength values for unbeaten black spruce kraft as a function of moisture content.

In contrast to Shallhorn's findings, work carried out by de Oliveira et al. [12], van de Ven [13] and Tejado and van de Ven [14] suggest that, in dry solids contents typical to the open draw from the press to the drying section and in the beginning of the drying section, capillary forces cannot be a major contributor to the wet strength. There must therefore be other forces present to provide wet tensile strength. The writers propose that entangled elastic fibres generate stress into the fibre crossings in a sheet, causing an entanglement friction that keeps the fibres in the sheet together and provides the wet tensile strength.

The entanglement friction mechanism can be conjectured based on the studies of Andersson et al. [15], Kulachenko et al. [3] and Huang et al. [16]. It has been noticed, especially in Atomic Force Microscopy (AFM) measurements, that friction force between fibres is the sum of the coefficient of friction multiplied by normal force and an initial tangent adhesive force that is independent of normal force [16, 17]. The initial tangent adhesive force arises due to the contribution of various attractive forces, such as capillary, electrostatic, van der Waals and chemical bonding under different circumstances [18]. Wet strength depends strongly on the extent of fibre-fibre interaction or number of inter-fibre contacts [1–3, 5, 10, 19–21].

Nanko's and Ohsawa's [22] experiments with beaten and unbeaten bleached Japanese beech kraft suggest that secondary fines fill the spaces between the fibres and, in addition, they form together with randomly orientated external macro and micro fibrils a more or less continuous bonding layer in the bonding areas between fibres. The macro fibrils lie mostly parallel to the fibre surface and they are not deeply entangled through the bonding zone [22]. Instead, it is likely that microfibrils are freer for entanglement and thus capable of increasing the entanglement friction. This supports the results of de Oliveira et al. [12] related to the effect of microfibrils.

Wet fibre surface can be considered as a gel-like layer of hydrated cellulose microfibrils and polymers with interactions between the microfibrils and polymers as well as between the adsorbed polymers [23–25]. For example, a random process of molecular motions could be expected to result in interpenetration and tangling of polymers on facing surfaces [24]. However, incompatible polymers cannot mix or interdiffuse during paper consolidation [26]. All these phenomena can be expected to affect the bonding mechanism of a wet web. It is conceivable that the effects are manifested as changes in the coefficient of friction and initial tangent adhesive force.

To conclude, the bonding mechanism in dry solids contents typical to the open draw after the press section and in the first part of the drying section is not fully understood. However, the entanglement friction has an important role in wet strength with the friction force and initial adhesion force acting on the fibre contacts. This kind of bonding mechanisms allows fibres to be detached, slide and attach again during deformation. Indeed, the modelling work of Kulachenko et al. [4] demonstrated that the deformation of the wet network is driven by continuous stick-slip behaviour at the fibre level. The same phenomenon is also visible in the results of Miettinen et al. [2]. As a comparison, in dry paper fibres are tightly bonded and the bonding mechanism does not allow the reattachment of fibres once the bonds are broken. Dissimilarities in the bonding mechanisms between the wet and dry fibre networks naturally lead to differences in deformation and breaking mechanisms.

2 METHODOLOGY

Trials were mainly carried out on the KCL AHMA pilot-scale strength testing machine for running paper webs [27]. In addition, one trial was run on the KCL pilot Fourdrinier where breaking tension and tensile stiffness (TS) were measured in situ with a wet web winder, installed right after the third press [28]. Consequently, all the strength properties were measured in the machine direction.

2.1 The KCL AHMA runnability pilot machine

The selection of KCL AHMA for the testing device was based on the following reasons:

- Compared with standard laboratory methods, web breaks occur under more realistic conditions as the web suddenly enters an open draw, where it experiences a rapid increase in tension.
- Specimen dimensions are large enough to enable the study of mesoscale structural effects as well as the effects of microstructure.

The device consists of the unwinder, notching device, three moistening units, storage path to control the web length from moistening to testing, special test draw section and shredding unit, cf. Figure 1. Pre-tensions (items 5, 8 and 11 in Figure 1) are controlled to the set values by speed differences from the unwinder to the brake nip. Web breaks occur in the one-meter long test section starting from the brake nip and ending at the pulling nip. The pulling nip repeatedly accelerates so that paper strain increases until the web breaks. The accelerating rate is controllable. The brake nip runs all the time at a constant speed. The web tension in the test draw is measured by two tension sensors integrated into the brake nip. One sensor is located on the tending side and the other on the driving side. The tension values and the respective strain values are recorded at 10 ms intervals. The device recovers automatically from a web break and the next acceleration ramp starts immediately after recovery. The automatic web break recovery uses rubber bands that carry the broken web into the pulling nip. The nip loads in the pulling and brake nips were 28 kN/m.

In order to reach low dry solids contents (DSC), a new rewetting procedure was developed. The first moistening unit consisting of a low pressure spray set with pump and flow control unit was installed by Metso Automation. In the system, the water is mixed with air at the nozzle exit, producing small water droplets. The water flow for each nozzle can be controlled independently from the other nozzles with rotameters. Altogether 12 nozzles were located in four rows enabling an even moisture profile. An embossed metal plate was installed to the opposite side of the web to support it in spraying, cf. Figure 2.

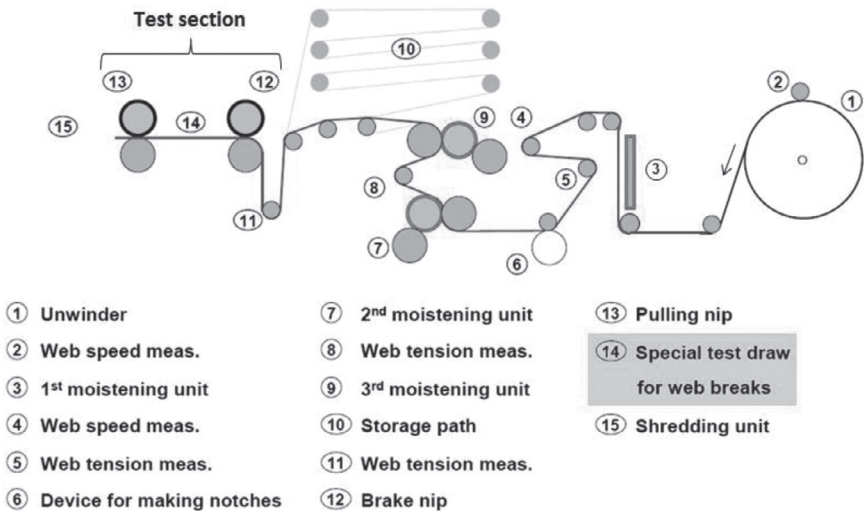


Figure 1. The main components of the KCL AHMA runnability pilot.

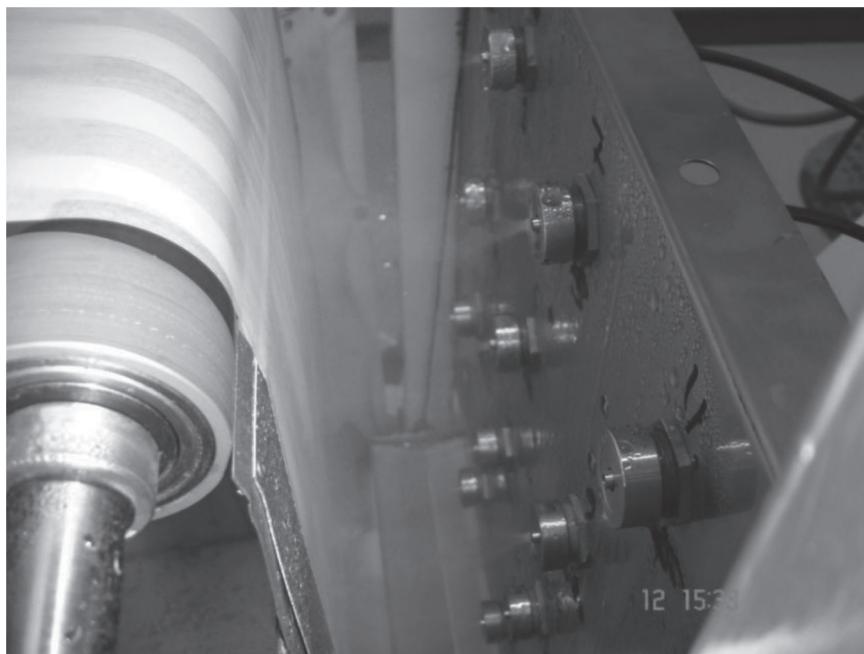


Figure 2. The spray unit (mounted between two white pillars).

The target dry solids contents were 56% and 68%. The spray was used together with the upper nip moistening unit to reach the lower target DSC. The nip load was 11.5 kN/m. Roughly half of the water was applied by the spray and half by the moistening nip. For the higher target DSC, the nip moistening was turned off but the nip was kept closed. In order to avoid picking, the lower moistening nip was kept open in all the runs. The web speed was 1 m/s allowing a delay of 12.2 s from the last spray nozzles to the test draw and 8.5 s from the upper moistening nip to the test draw. Distilled water was used in all the runs. These arrangements were considered adequate enough to restore dry unsized paper webs close to the condition of newer dried ones enabling therefore the usage of dry mill made paper reels [29].

2.1.1 The effect of pre-straining of the wet web before the test section

Because the total strain from the unwinder to the pulling nip was not available, the effect of pre-straining on tensile strength and tensile stiffness values is evaluated based on the on the following experiments.

Tanaka et al. [28] compared the strength properties measured in situ using the wet web winder and KCL AHMA. The wet reels for the runnability pilot were wound on the wet web winder and transported to AHMA for measurements. According to their results, the wet tensile strength measured with both methods was the same irrespective of the type of furnish. Instead, breaking strain values measured on AHMA were much smaller and tensile stiffness higher than those measured directly from the press section. The likely explanation is the straining history which was different for the web on the pilot paper machine and on AHMA because before the test section the web had already experienced about 2.5% straining on the wet web winder plus straining due to the pre-tension on AHMA. However, the results of Tanaka et al. [28] suggest that at certain moisture content the total breaking strain, consisting of the strain on the pilot paper machine, pre-strain on AHMA and strain in the test section, turned out to be quite independent of the pre-tension (42 N/m or 208 N/m) and running speed on AHMA.

Barnet and Harvey [30] explored the properties of a wet web on a pilot paper machine running at 55 m/min. The furnish was a mixture of TCMP and GW. The web was sampled in three open draws for testing. Their results support the independence of the total strain from the straining history, see Table 1.

Mäkinen [31] produced wet LWC base paper reels on a 700 m/min running hybrid pilot paper machine equipped with a shoe press and one ordinary nip press. The DSC of the final paper was approximately 49%. The wet draw over the machine was varied approximately between 5.3% and 8.6% with the changes being made between the first press and the dryer. The wet reels were transported to AHMA for strength measurements. The increase in the wet draw on the pilot paper machine was only partially compensated by the reduced breaking strain on AHMA, with the outcome being a clear difference in the total breaking strain, see Table 2. However, in spite of a significant increase in the paper machine draw, the wet tensile strength remained practically unchanged (difference 3.9%). Tensile stiffness naturally increased due to the reduced breaking strain and fairly constant tensile strength on AHMA.

Table 1. Total break strain with different straining combinations. The results are recalculated from the results of Barnet and Harvey [30].

<i>Couch draw %</i>	<i>1st press draw %</i>	<i>2nd press draw %</i>	<i>Draw to break at</i>	<i>Draw to break %</i>
7.1			couch	7.1
2.6	4.2		1st press	6.8
2.6	2.1	2.5	2nd press	7.2

Table 2. The effect of wet straining on a pilot paper machine (PM) on the total strain, tensile strength and tensile stiffness of the wet web. The breaking strain on AHMA includes the strain (0.7–0.8%) due to the pre-tension. Results are recalculated from the results of Mäkinen [31].

<i>Draw over pilot PM %</i>	<i>Breaking strain on AHMA, %</i>	<i>Total breaking strain %</i>	<i>Tensile strength kN/m</i>	<i>Tensile stiffness kN/m</i>
5.3	3.3	8.6	184	8.1
8.6	2.0	10.7	191	10.1

The results above suggest that the tensile strength of the wet web is independent of the wet straining history. In addition, the same also seems to be valid for the total breaking strain when the variation in the wet straining history is not large. If pre-straining is fairly constant between trial points, the stretch-at-break and tensile stiffness values measured on the test section of AHMA in different trial points are comparable with each other, although at a different level with the in situ measurements on a paper machine. Pre-tensions in our trials were low and constant, 80 N/m in the first and second measurement point (items 5 and 8 in Figure 1) and 88 kN/m in the third measurement point (item 11).

2.2 Trial papers

The middle position reels for the AHMA trials were collected from the paper mill winders. Reels initially 55 cm wide were slit to 25 cm wide at KCL.

Table 3 shows the trial papers. Papers News 1–6 were manufactured on a roll-blade gap former consisting of a “constant dewatering” zone by the forming roll wrap area followed by a “pulsating dewatering” zone of a multifoil shoe. Paper was manufactured by changing forming roll vacuums (2/4–12/15 kPa), multifoil shoe vacuums (2/3–8/15 kPa), slice opening (6.8–7.5 mm) and jet-to-wire ratio (1.045–1.075). The unity point (change from rush to drag) was 1.015. The total draw from the wire to the reel-up was 5.7%. Furnish was kept as constant as possible.

With the selected parameters it is possible to affect the drainage and flow field of the suspension in the dewatering zone [32–35]. Each individual section in the z-direction of the web forms in different locations along the forming zone. Therefore the layers may have experienced very different forming history presenting the possibility of producing various paper structures. Fibre orientation throughout the whole thickness of the sheet is affected as a minimum. LWC base papers were taken from a normal production from two LWC mills, mill A and mill B.

Table 3. Newsprint and LWC base papers used in AHMA trials and run on a pilot Fourdrinier. RCF denotes recycled fibres. RBG denotes roll-blade gap former and LB denotes loadable blades. All the papers were unsized.

<i>Papers</i>	<i>Grade</i>	<i>Basis weight</i>	<i>Furnish</i>	<i>Former</i>
N1–N6	News	45	RCF	RBG
A1	LWC	40	TMP/kraft	RBG
A2–A3	LWC	40	TMP/kraft	RBG & LB
B1–B2	LWC	48	PGW/kraft	RBG
Pilot1–Pilot4	News	58	TMP	Fourdrinier

In order to have a larger formation range for analyses, four trial papers with poor formation were included in the study. The papers, basis weight 56.6–58.9 g/m², were manufactured on a pilot Fourdrinier from 100% TMP. Furnish was the same for all four trial papers. Formation was altered with headbox consistency and wire section vacuums. Fibre orientation was almost constant. The dry solids content was 40%.

2.3 Structure measurements

2.3.1 Formation measurements

The formation results are based on a β -radiographic method using a reusable storage phosphor screen (SPS) and β -radiation (¹⁴C) source [36]. The image on the screen was digitised into a matrix of grey level data using a Fuji BAS-1800 II SPS scanner. The resolution was 50 $\mu\text{m}/\text{pixel}$ and the size of the grammage map was 120 mm \times 120 mm. Grammage variation is examined as standard deviation in the following wavelength ranges: 0.25–2, 2–8 and 8–32 mm. The range of 0.25–32 mm is referred to as total formation. In addition, formation was also measured with Ambertec formation tester.

In order to get a more comprehensive picture of the paper structure, void distribution was studied by utilising Matlab Image Processing ToolboxTM. Median thresholding and a few morphological operations [37] were employed. The pixels whose value was at least 4 g/m² smaller than the median value were considered to belong to voids. The effect of voids is examined by measuring the total area of voids belonging to size classes 1–8 mm² and 8–16 mm² (also over 8 mm² in the case of the pilot papers).

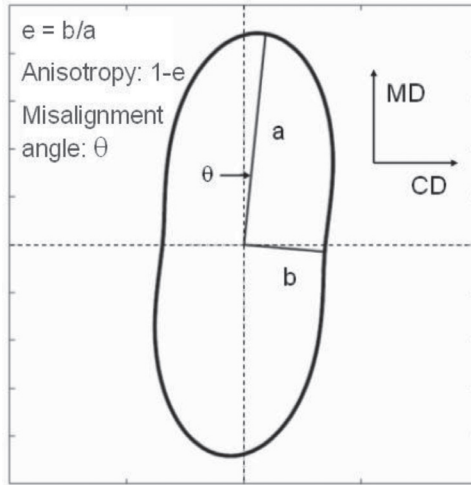


Figure 3. Orientation distribution pattern and parameter definition, Erkkilä [32].

2.3.2 Fibre orientation measurements

Fibre orientation was determined using layered fibre orientation measurements [32, 38]. The method is based on the tape-stripping technique and image analysis of the resulting layers. The stripping procedure was done according to the reference [39]. The average grammage and max-min range for the layers were fairly similar in all the tested papers, with typical values being 5 g/m^2 and $3.3\text{--}6.2 \text{ g/m}^2$ respectively.

Each specimen layer was placed against a dark background and scanned with the UltraScan 5000 flatbed scanner from the fibre side with $30 \text{ }\mu\text{m/pixel}$ resolution using reflective illumination. The fibres and fibre bundles are distinguished as lighter against the dark background. In the image analysis, intensity variations are sharpest at the fibre boundaries. This result is used in the form of gradients to establish the magnitude and direction of fibres in every image element throughout the whole image area. Three areas of $180 \text{ mm} \times 40 \text{ mm}$ ($\text{CD} \times \text{MD}$) were measured from every layer. By plotting the result for each layer using polar co-ordinates, an ellipse-type of fibre orientation distribution pattern is obtained, Figure 3.

Two types of orientation results are discussed. In order to determine ZD anisotropy profile average anisotropy and misalignment angle was computed for every layer. In addition, anisotropy ($1 - e$) for the whole paper was computed as a mass-weighted average.

With both axes being equal, the anisotropy is 0. The maximum value for anisotropy is 1 when all the fibres are oriented to the direction of the major axis.

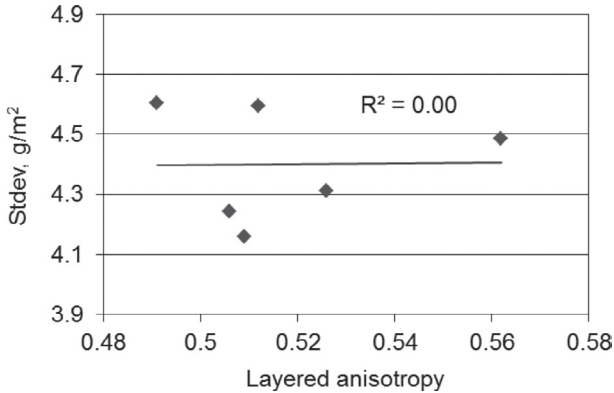


Figure 4. Correlation between total formation (wavelength band 0.25–32 mm) and layered anisotropy. β -radiography.

3 RESULTS

3.1 Possible correlation between formation and fibre orientation

In order to distinguish between the effects of formation and fibre orientation on the strength properties, the variables should not be correlated. To clarify whether this was the situation for the News series N1–N6, an investigation was conducted by means of visual evaluation of the charts and statistical methods. Based on the results, there was no statistically significant correlation at a 95% confidence level, not even at 90%, between layered anisotropy and local grammage variation in different wavelength bands or void size classes or Ambertec formation, and there was no correlation based on visual evaluation either, cf. Figure 4. The result is understandable because formation was not altered only by the jet-to-wire ratio.

In contrast to the News series, fibre orientation and formation correlated with each other in LWC base papers because it was not possible to control the mentioned properties separately during manufacturing. Due to this reason the discussion on the effect of paper structure on strength properties in mill made papers is restricted to the Newsprint series only.

3.2 The effect formation and fibre orientation on average strength properties

3.2.1 Formation

The parameter combination enabled a considerably large formation range. It was 4.16–4.60 g/m² based on β -radiography and 2.9–3.4 g/m² according to Ambertec

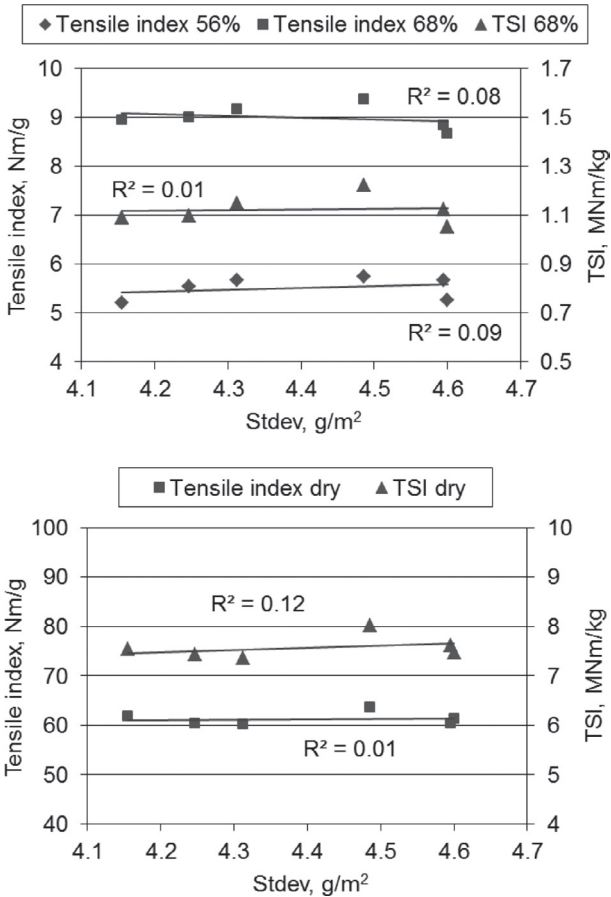


Figure 5. Tensile index and tensile stiffness index as a function of local grammage variation (β -radiography, wavelength band 0.25–32 mm). 56% and 68% denote dry solids contents. News series.

measurements. The range is large at this formation level, especially because the employed parameters were headbox and wire section settings only.

Figure 5 suggests that local grammage variation does not correlate with wet or dry tensile index and TSI. Visual evaluation of the charts and statistical investigation confirmed this. Strength properties were correlated with total formation (Ambertec, β -radiography) and grammage variation in different wavelength bands and void size classes.

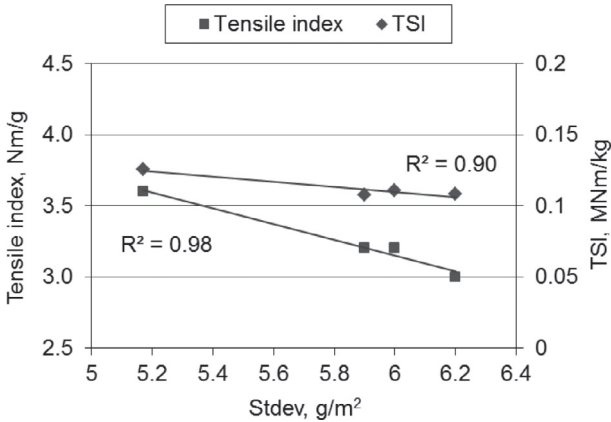


Figure 6. Tensile and tensile stiffness indices as a function of local grammage variation (Ambertec). DSC 40%.

TSI was determined only for DSC 68% and for dry papers. The reason is that the initial tension in the test draw (item 14 in Figure 1) needed to be fairly high, on average 175 N/m, in order to allow the acceleration of the pulling nip after web breaks. Consequently, the difference between the breaking tension and initial tension remained fairly small at a DSC of 56%. Thus the measured tension-strain curves would represent only a fraction of the real tension-strain curves, bringing the relevance of the usage of the slope as an indicator for TSI into question. The situation was quite different at DSC 68% due to higher breaking tension values.

Contrary to the News results (from a roll-blade gap former), where the formation was at a good level, the pilot results (from a Fourdrinier type of former) suggest that when the formation is poor, i.e. the formation number has a high value and the web structure is cloudy, this has a negative effect on wet tensile and tensile stiffness indices, cf. Figure 6.

Table 4 and Figure 7 demonstrate that the differences between the Fourdrinier-made and gap former-made papers are substantial. For example, the widest max-min difference between the pilot papers appears to be in wavelength band 8–32 mm, whereas it is in wavelength band 2–8 mm for all other papers tested.

Interestingly, in the pilot papers the total void area in the size class over 8 mm² and the basis weight variation measured at the wavelength band of 8–32 mm, which both describe a large-scale formation variation, provided the strongest correlations with the wet tensile index, cf. Figure 8. In addition, the correlation was almost statistically significant at a 95% confidence level for the wavelength band 8–32 mm (p value 0.057).

Table 4. Differences in formation between pilot papers 1–4 (Fourdrinier) and News N1–N6 (roll-blade gap former). Average values and Max-Min differences in three wavelength bands. β -radiography measurements only from three pilot papers.

Paper	<i>A-tec, g/m²</i>		β -radiography, g/m ²		
	<i>Average</i>	<i>Average</i>	<i>0.25–2 mm Max-Min</i>	<i>2–8 mm Max-Min</i>	<i>8–32 mm Max-Min</i>
News	3.2	4.40	0.19	0.49	0.31
Pilot	5.8	6.63	0.37	0.61	0.67

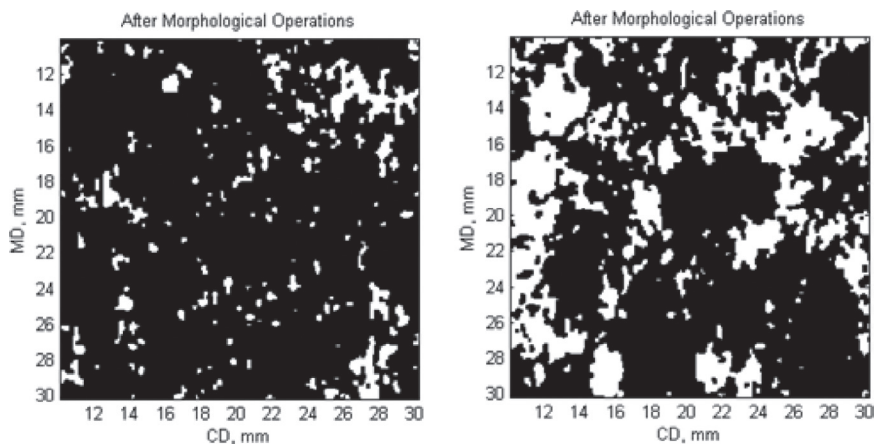


Figure 7. Examples of formation. Image analysis based on β -radiography. White areas are voids, thresholding: median – 4 g/m². The images are 20 mm × 20 mm segments from the original 120 mm × 120 mm radiograms. Left: News N5. Right: Pilot paper 2.

3.1.2 Fibre orientation

The trial papers can be separated into two different categories according to the anisotropy profile in z-direction. Papers 3 and 6, manufactured with a high jet-to-wire ratio, show a symmetric two maximums type of anisotropy profile around the sheet centre, cf. Figure 9. This type of anisotropy profile is typical for roll-blade gap formers running in rush [33, 38, 40]. The four other trial papers, run with the lower jet-to-wire ratio of 1.045, demonstrate a more or less asymmetric profile type with one maximum. The one maximum type of profile is typical for running

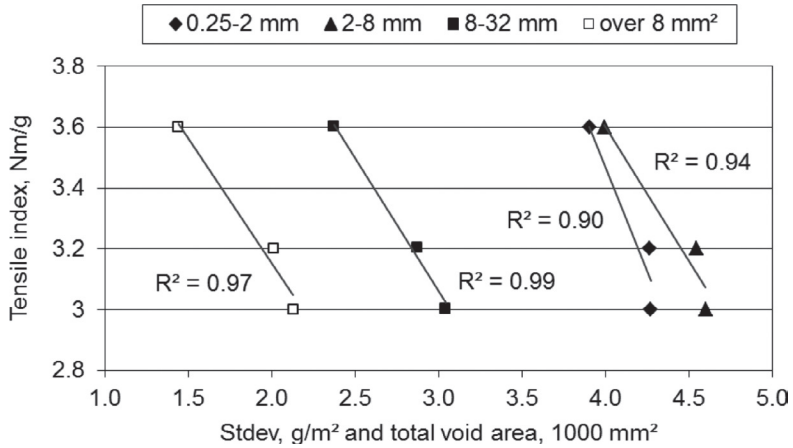


Figure 8. The effect of different formation size ranges on the wet tensile index. β -radiography. The total area of voids belonging to the size range over 8 mm² is measured from the area of 120×120 mm². Pilot papers at DSC 40%.

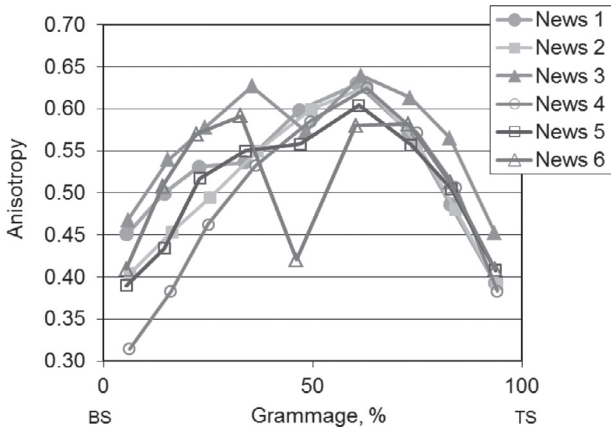


Figure 9. Anisotropy in different paper layers starting from the bottom side. News series.

in drag. However, achieving this type of profile while running in rush is not a unique phenomenon. For example, in Erkkilä's study [32] on a pilot and a production roll-blade gap former the anisotropy profile changed from the two maximums type to a more or less asymmetric one maximum type when the jet wire ratio was reduced close to the unity point.

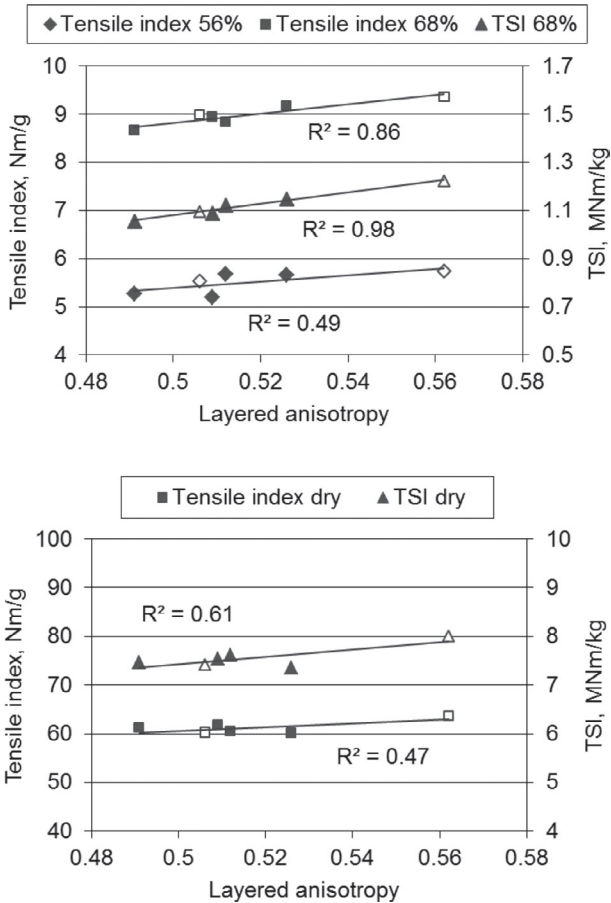


Figure 10. Tensile and tensile stiffness indices as a function of layered anisotropy. The open symbols denote two maximums type of anisotropy profile in z-direction and solid symbols one maximum type of profile. News series.

The misalignment angle profile in the z-direction was very even in all the trial papers with the average angle varying from layer to layer between -3° and $+3^\circ$. Therefore there are no practical differences between the papers.

As regards to the two different types of profiles, Figure 10 suggests that the anisotropy profile in z-direction has no influence on the tensile strength or tensile stiffness of wet and dry papers. Instead, the total anisotropy affects the mentioned strength properties. The effect is especially significant in the tensile stiffness

index at a DSC of 68%. Another interpretation is that from the wet and dry tensile strength and tensile stiffness point of view it does not matter whether the machine runs in the rush or drag side.

Kouko et al. [8] showed that fibre orientation correlates with tensile strength and residual tension in wet paper (DSC 44%). Thus the result supports our findings.

3.2 Strength distributions

Evidently, the strength distribution and failure phenomenon are interrelated. For example, in dry paper the rupture mechanism leads to extreme value statistics [41, 42]. Typically, the tensile strength of dry paper can be described by means of the two-parameter Weibull distribution [41, 43–45]. Instead, it is not known whether the strength distribution of wet paper can be described by any extreme value distribution at all. The issue was studied by fitting the Weibull (1), Gumbel for minimum (2) and Gaussian distribution (3) to the measured data.

$$W(x) = 1 - \exp \left[- \left(\frac{x}{\alpha} \right)^\beta \right] \quad (1)$$

where

$W(x)$ is the cumulative failure probability at tension x

β is the shape parameter

α is the scale parameter.

$$G(x) = 1 - \exp \left[- \exp \left(\frac{x - \mu}{\alpha} \right) \right] \quad (2)$$

where

$G(x)$ is the cumulative failure probability at tension x , cf. Appendix 1

μ is the location parameter

α is the scale parameter.

$$N(x) = \int_{-\infty}^x \frac{1}{\sigma\sqrt{2\pi}} e^{-\frac{(t-\mu)^2}{2\sigma^2}} dt \quad (3)$$

where

$N(x)$ is the cumulative failure probability at tension x

μ is the location parameter

σ the scale parameter.

The parameter fitting and selection of the best model was performed using Akaike's Information Criterion (AIC) [46, 47] (4).

$$AIC = -2\log(L(\hat{\theta})) + 2K \quad (4)$$

where

\log denotes natural logarithm

$\log(L(\hat{\theta}))$ is the maximised value of the log-likelihood function $\log(L(\theta))$

$L(\theta)$ is the likelihood function of the estimable model parameters θ , given the data and the model g_i

K is the number of estimable parameters in a candidate model.

AIC values and maximum likelihood estimates were computed with Matlab for each of the candidate distribution models g_i using Wafo toolbox [48]. The model with the smallest value of AIC was selected as best. This model is estimated to be “closest” to the unknown reality that generated the data [47].

The value of the maximised log-likelihood (i.e. $\log(L(\hat{\theta}))$) and the value of AIC varies substantially from sample to sample, cf. Table 5. For example, sample size and the absolute values of data points have an influence here. However, all the comparisons of models are made using the same data, making the sample-to-sample variation irrelevant. This all means that it is the AIC differences (Δ_i) between the distribution models that are important, not the absolute magnitudes [47]. AIC differences were computed according to formula (5).

$$\Delta_i = \text{AIC}_i - \text{AIC}_{\min} \quad (5)$$

The significance of AIC differences is based on the following rough rules provided Burnham and Anderson [47].

Δ_i	Level of empirical support on model
0–2	Applicability of the model is substantially the same with the best model
4–7	Considerably less support for the applicability of the model
>10	Essentially no support for the applicability of the model.

Table 5 shows both computed AIC values and AIC differences. A grey scale code, based on the guidelines above, was established to visualise possible differences between the Gaussian and extreme value distributions. As the table shows, there is strong evidence that, at the lowest DSC of 56%, tensile strength is distributed normally and both the extreme value distributions, two-parameter Weibull and Gumbel to minimum, provide a poor fit to the actual strength distribution, cf. Figure 11 as an example.

Based on AIC differences, the Gaussian distribution also provides a better fit at the higher DSC of 68% although the performance of all the distributions of the newsprint series starts to resemble each other. According to visual evaluation, however, the Gaussian distribution provides a better fit at the low end of the strength distribution. The LWC base papers show stronger Gaussian behaviour at DSC 68% than the newsprint series based on AIC values and visual evaluation. However,

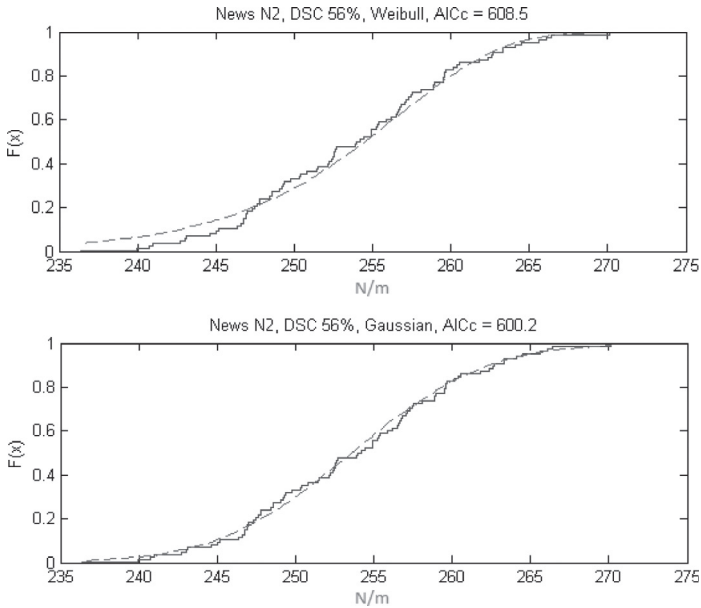


Figure 11. An example of measured (solid line) and modelled (dash line) cumulative tensile strength distributions. DSC 56%. News N2.

Gaussian behaviour also weakened in their case according to AIC differences; only two papers out of five show strong Gaussian behaviour instead of four at DSC 56%.

The final piece of strong evidence in favour of the Gaussian distribution for wet papers is that it has the smallest AIC value 21 times out of 22.

According to AIC difference, both the extreme value distributions seem to perform fairly equally in dry papers. In addition, based on a visual evaluation of the distributions fitted to the data of all dry papers, it is impossible to give any priority to either of the extreme value distributions when both the low tail and middle area of the distributions are considered.

Based on the results above, it is suggested that the tensile strength of wet paper—at least at dry solids contents typical to the press section and the first part of the drying section—is normally distributed instead of any extreme value distribution.

3.3 The effect of paper structure on the strength distribution of wet and dry paper webs

In this chapter, the aim is to study what kind of effects paper structure has on the tensile strength distribution of wet and dry papers. Possible effects are measured

Table 5. AIC differences (Δ_i) and AIC values for News series N and LWC base paper series A and B. White = substantial evidence that both Gaussian and extreme value distributions can be used to describe the strength data. Light grey = considerably less support for that. Dark grey = it is very unlikely that both Gaussian and extreme value distributions are suitable choices.

<i>Dry Solids Content 56%</i>						
<i>Data Set</i>	<i>A_i</i>			<i>AIC</i>		
	<i>Weibull</i>	<i>Gumbel</i>	<i>Gaussian</i>	<i>Weibull</i>	<i>Gumbel</i>	<i>Gaussian</i>
N1	8.8	10.3	0	552.5	554	543.7
N2	8.3	9.9	0	608.5	610.1	600.2
N3	16.1	18.5	0	585.8	588.2	569.7
N4	19.7	22.3	0	698	700.6	678.3
N5	1.6	2.5	0	550.1	551	548.5
N6	5.7	6.8	0	394.1	395.2	388.4
A1	0.6	1	0	361.1	361.5	360.5
A2	17.9	19.7	0	419.2	421	401.3
A3	21.3	23.3	0	424.4	426.4	403.1
B1	11.7	13.6	0	371	372.9	359.3
B2	8.3	10.2	0	524.7	526.6	516.4

<i>Dry Solids Content 68%</i>						
<i>Data Set</i>	<i>A_i</i>			<i>AIC</i>		
	<i>Weibull</i>	<i>Gumbel</i>	<i>Gaussian</i>	<i>Weibull</i>	<i>Gumbel</i>	<i>Gaussian</i>
N1	0.4	1.7	0	758.3	759.6	757.9
N2	2.8	4.3	0	736.8	738.3	734
N3	1.2	2.9	0	892.5	894.2	891.3
N4	0.9	3	0	752.2	754.3	751.3
N5	0	0.6	5.4	714.9	715.5	720.3
N6	16.4	19.1	0	807.2	809.9	790.8
A1	4.3	5.5	0	608.1	609.3	603.8
A2	19.1	22.1	0	656.8	659.8	637.7
A3	6.5	7.7	0	672	673.2	665.5
B1	7.2	9.2	0	586.7	588.7	579.5
B2	10.6	12.8	0	796.5	798.7	785.9

Dry

Data Set	Δ_i			AIC		
	Weibull	Gumbel	Gaussian	Weibull	Gumbel	Gaussian
N1	1.6	0	40.4	1149	1147.4	1187.8
N2	7.6	0	71.4	1190.9	1183.3	1254.7
N3	5.8	0	65.9	1218.9	1213.1	1279
N4	0	0	13.5	1118.8	1118.8	1132.3
N5	2.8	0	52	1159.3	1156.5	1208.5
N6	0	0.5	8.3	1136.5	1137	1144.8
A1	0.2	0	17.4	1104.3	1104.1	1121.5
A2	4.5	6.4	0	1182.9	1184.8	1178.4
A3	0	0.1	11.1	1125	1125.1	1136.1
B1	0	0.7	4	1273.5	1274.2	1277.5
B2	0	2.1	0.7	1238.5	1240.6	1239.2

as a change of coefficient of variation (COV) and Weibull shape parameter (Weibull modulus). However, the latter is computed for dry papers only. Paper structure is described by means of fibre orientation and local basis weight variation in different wavelength bands and void size classes.

According to Table 6, COV is smaller and varies considerably less between the papers at a DSC 56% compared with the situation at other dry solids contents.

Table 6. COV computed as an average for the tensile index of News and LWC base papers. Max-Min denotes the maximum COV difference between the papers in each paper group. The weighted averages (WA) are computed by weighting the averages by the number of papers in each paper group.

	DSC 56%		DSC 68%		Dry	
	COV	Max-Min	COV	Max-Min	COV	Max-Min
News N1–N6	2.70	0.25	3.31	1.11	4.05	3.97
LWC base A1–A3	2.14	0.15	2.70	0.58	3.23	0.48
LWC base B1–B2	3.39	0.09	3.56	0.55	3.43	0.36
COV, WA	2.67		3.19		3.71	
Skewness, WA	0.19		-0.15		-1.37	

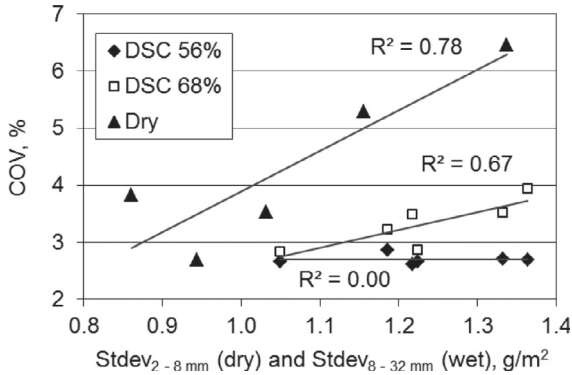


Figure 12. Coefficient of variation of tensile index as a function of local basis weight variation in wavelength bands 8–32 mm (wet papers) and 2–8 mm (dry papers). β -radiography. All the formation values of dry papers are deducted by 1.5 g/m² in order to accommodate both wavelength bands in the same figure. Newsprint.

The smaller variation is evident when comparing the Max-Min values. The results suggest that web strength is remarkably uniform in the wet state. This confirms the simulation results of Kulachenko and Uesaka [49]. The skewness values indicate the strength distribution to turn from Gaussian into a left tailed extreme value distribution as paper dries and the bonding mechanism changes. This result is consistent with the results shown in Table 5.

Because COV between papers varied only slightly at a DSC of 56%, it is understandable that no statistically significant correlation was found between COV and formation parameters, cf. Figure 12. Instead, formation seems to have a significant effect on the strength variation at a DSC of 68% and in dry paper. Interestingly, the results suggest that the intensity of the effect depends both on the scale of formation and on DSC (no effect at DSC 56% and the greatest effect in dry papers), cf. Table 7 and Figure 12. At a DSC of 68%, correlation becomes stronger when the scale of formation increases. Finally, on the large scale—wavelength range 8–32 mm and total void area in size class 8–16 mm²—correlation is statistically significant at a 95% confidence level. Conversely, in dry papers correlation is strongest on the wavelength band 2–8 mm.

The results of dry paper are congruent with the results of Hristopulos and Uesaka [41] who showed formation on the length scale smaller than a few mm to have an effect on the tensile strength variation of dry paper.

Contrary to formation, fibre orientation does not influence the strength distribution of wet or dry paper (cf. Table 7 and Figure 13) although it has an effect on average strength values as shown earlier.

Table 7. Correlation coefficients and respective p values for the correlations between structural parameters and COV and Weibull modulus β for the tensile index. Highlighted correlations are statistically significant at a confidence level of 95%. Newsprint

	COV DSC 68%		COV dry		Weibull modulus, dry	
	p value	R	p value	R	p value	R
Layered anisotropy	0.791	-0.14	0.580	0.34	0.544	-0.37
β -radiography	0.064	0.79	0.048	0.88	0.027	-0.92
β -radiography _{0.25-2 mm}	0.303	0.51	0.281	0.60	0.215	-0.67
β -radiography _{2-8 mm}	0.063	0.79	0.045	0.89	0.028	-0.92
β -radiography _{8-32 mm}	0.047	0.82	0.053	0.87	0.069	-0.85
Voids _{1-8 mm} ²	0.232	0.58	0.084	0.83	0.059	-0.87
Voids _{8-16 mm} ²	0.037	0.84	0.162	0.73	0.212	-0.68

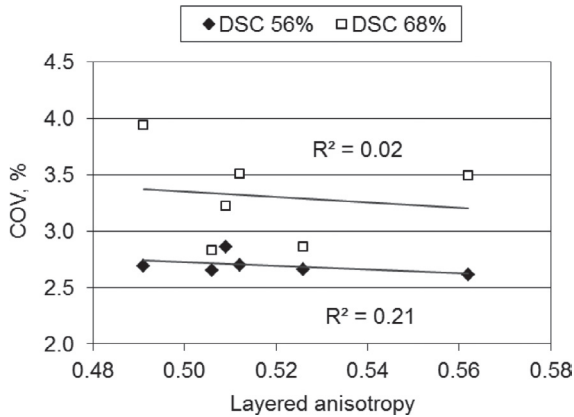


Figure 13. Coefficient of variation of tensile index as a function of layered anisotropy. Newsprint.

3.4 Effect of defects

The effect of defects was tested by making 2 cm wide CD notches in the middle of the web. The notch-making device was located in the AHMA runnability device between the spray unit and the lower nip moistening unit, item 6 in Figure 1. Irrespective of furnish, formation and fibre orientation notches did not have any effect on the tensile strength of wet papers, cf. Figure 14. The result is

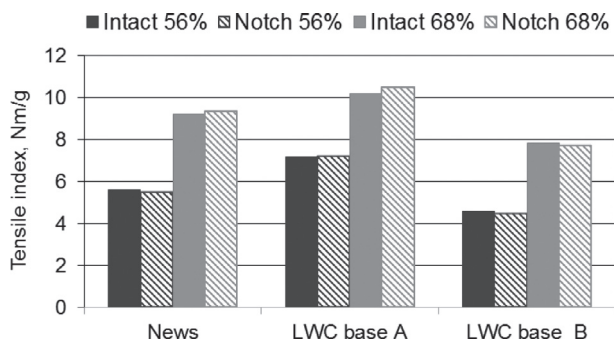


Figure 14. Breaking tension of webs affected by 2cm wide CD centre notches compared with intact webs. DSC 56% and 68%. Newsprint series and LWC base paper series A and B.

understandable on the grounds of the capability of the wet fibre network to effectively even out the tension peaks caused by defects.

4 DISCUSSION

The developed remoisterizing procedure enabled the testing of rewetted mill made paper reels on the pilot-scale runnability device, KCL AHMA. In order to differentiate between the effect of formation and fibre orientation on strength properties, the variables should not be correlated. This requirement was met in the main mill trial by suitably selecting the headbox and wire section parameters.

At a DSC of 56% the tensile strength of mill made papers was shown to be remarkably uniform. This finding is congruent with the fibre level network simulation results [4, 49]. The uniform strength field in wet paper is understandable on the grounds of the bonding mechanism. It is suggested that in wet paper, bonding between the fibres is based on entanglement friction [12–14] with the friction force and initial tangent adhesion force acting on the fibre contacts [15–17] allowing the wet sheet to deform by continuous stick-slip behaviour on the fibre level [2, 4]. In this type of deformation mechanism, the wet network can easily adapt and even out the external load. However, the developing strain field is uneven [4, 50].

The simulation results of Kulachenko and Uesaka [49] and experimental work of Borodulina [51] suggest the strain field to develop as a form of shear bands, typical to many ductile materials. At the beginning of loading, in the linear region of the tensile stress-strain curve, the strain field shows a presence of a distinct non-

uniform diagonal “criss-cross” pattern. While the external load increases, the slippage starts to localize and some nucleation emerge. Finally, there exists a clear localization of failure across the fibre network and most of the slippage between the fibres occurs in this region and the wet web breaks. It is understandable that the described deformation mechanism leads to the Gaussian distribution. The result, that notches did not have any effect on the tensile strength of wet papers, confirms that in the wet web the rupture process does not initiate from a single weak spot.

Because wet strength depends strongly on the extent of fibre-fibre interaction or number of inter-fibre contacts [1–3, 5, 10, 19–21], it is conceivable that formation has an effect on the distribution of inter-fibre contacts and via that, an effect on the magnitude and uniformity of shear bands and the nucleation of damages. This could explain why formation had an influence on the average tensile strength of pilot papers but not on that of Newsprints. The reason is suggested to be the very poor large scale formation of the pilot papers, cf. Figure 7. This kind of uneven and large thin areas containing structure presumably brings forth damage nucleation and failure location at an early stage of loading compared with the more even structure of Newsprints.

The distribution results suggest that at both dry solids contents, 56% and 68%, the strength of paper is normally distributed, although the difference between the Gaussian and extreme value distributions mitigates when DSC increases. Finally, the strength distribution in dry papers can be described by an extreme value distribution. The gradual change of the strength distribution can be understood on the grounds of the bonding and deformation mechanisms. When DSC increases, hydrogen bonds start to emerge until, in the dry paper, fibre bonds are largely formed by hydrogen bonding accompanied by van der Waals’ forces [52]. The deformation and rupture mechanisms of paper naturally change accordingly. The dry solids content at which actual interfibre bonds form is not exactly known. However, in the case of kraft pulp it is approximately at 50% DSC [52]. This means that, at least at the higher dry solids content of 68% hydrogen bonds contribute to some degree to wet strength properties. It is suggested that individual fibres cannot slide in relation to each other as freely as at the lower DSC of 56%. Therefore formation starts to have an effect on the strength distribution. But again, it is the large scale formation that matters, cf. Table 7.

The deformation phenomenon of dry papers can be considered based on the studies of Wong et al. [53] and Korteoja [42]. Their results suggest that paper formation affects the way external elongation is distributed through paper into local strains. The low grammage points accumulate far more strain, and consequently more damage, than high grammage points. Thus the damage accumulates in low grammage points throughout the whole paper specimen or paper web but the final rupture process always starts from a single weak spot and paper breaks abruptly. It is natural to expect this kind of rupture mechanism to lead to an extreme

value strength distribution. The simulations of Korteoja [42] suggest that plastic deformation in dry paper takes place in less than a quarter of the paper area when paper is loaded. Increased formation-type disorder reduces this fraction.

The results of Borodulina et al. [51] confirm that large local strain concentrations are the precursors of bond failures. Only a minor percentage of bonds fail completely before the rupture [51, 54]. The width of strain concentration regions have a size on a millimetre scale and obviously depend on the initial details of the network structure [51]. This would explain why small scale formation, length scale a few mm, turned out to have dominating influence on the strength variation of dry paper according to our results and the results of Hristopulos and Uesaka [41].

5 CONCLUDING REMARKS

The employed pilot-scale procedure provides a good means to study the wet strength properties of mill made papers at low dry solids contents.

It is evident that the dry solids content, bonding and failure mechanisms and strength distribution are closely interrelated.

In contrast to dry strength, the wet strength does not follow the Weibull distribution, but rather the Gaussian one. In addition, the strength is remarkably uniform in a wet state showing only minor strength variations. Further, the distribution of wet strength is sensitive to centimetre-scale variability in paper structure instead of millimetre-scale in dry paper.

When formation is good, as it typically is on modern paper machines, further improvement does not improve average wet strength properties. Only when large scale formation is poor, does this have an influence on average wet web tensile strength and tensile stiffness. Presumably this would be the situation on a Fourdrinier type machine.

Contrary to formation, anisotropy does not affect the strength variation but it has an influence on the average tensile strength and tensile stiffness of wet and dry papers. Instead, the anisotropy profile in z-direction has no influence on the mentioned properties.

The wet web tensile strength is insensitive to defects, at least if they are not located just at the edge of the web.

REFERENCES

1. P.P.J. Miettinen, J.A. Ketoja and T. Hjelt. Simulated structure of wet fiber networks. *Nordic Pulp and Paper Research J.* **22**(4):516–522, 2007.

2. P.P.J. Miettinen, J.A. Ketoja and D.J. Klingenberg. Simulated strength of wet fibre networks. *Journal of Pulp and Paper Science*. **33**(4):198–205.
3. A. Kulachenko, T. Uesaka and S. Lindström. Reinventing mechanics of fibre network. In proc. *Progress in Paper Physics Seminar 2008*, pp185–187, 193, Espoo, Finland. Helsinki University of Technology (TKK), Espoo, 2008.
4. A. Kulachenko, S. Lindström and T. Uesaka. Strength of wet fiber networks – Strength scaling. In proc. *Papermaking Research Symposium*, 10p, Kuopio, Finland. University of Kuopio, Kuopio, 2009.
5. S.B. Lindström, A. Kulachenko and T. Uesaka. New insights in paper forming from particle-level process simulations. In proc. *Papermaking Research Symposium*, 10p, Kuopio, Finland. University of Kuopio, Kuopio, 2009.
6. C. Yang and J. Thorpe. Density distribution vs. wet strain in paper sheets. *Tappi J.* **60**(12):141–145, 1977.
7. J. Thorpe and C. Yang. The influence of local variation in grammage on wet web straining of newsprint. *Svensk Papperstidning*. **82**(7):207–211, 1979.
8. J. Kouko, K. Salminen and M. Kurki. Laboratory scale measurement procedure for the runnability of a wet web on a paper machine, Part 2. *Paperi ja Puu*. **89**(7–8):424–430, 2007.
9. W.B. Campbell. The cellulose-water relationship in papermaking, Bulletin (Canada. Dominion Forest Service), no. 84. Printer to the King's most excellent Majesty, Ottawa, 1933.
10. D.H. Page. A quantitative theory of the strength of wet webs. *Journal of Pulp and Paper Science*. **19**(4):J175–J176, 1993.
11. P.M. Shallahorn. Effect of moisture content on wet-web tensile properties. *Journal of Pulp and Paper Science*. **28**(11):384–387, 2002.
12. M.H. de Oliveira, M. Maric and T.G.M. van de Ven. The role of fiber entanglement in the strength of wet papers. *Nordic Pulp and Paper Research J.* **23**(4):426–431, 2008.
13. T.G.M. van de Ven. Capillary forces in wet paper. *Industrial and Engineering Chemistry Research*. **47**(19):7250–7256, 2008.
14. A. Tejado and T.G.M. van de Ven. The strength of wet paper: Capillary forces or entanglement friction? In proc. *7th International Paper and Coating Chemistry Symposium*, pp51–56, Hamilton, Canada. PAPTAC, Montreal, 2009.
15. S.R. Andersson, T. Nordstrand and A. Rasmuson. The influence of some fibre and solution properties on pulp fibre friction. *Journal of Pulp and Paper Science*. **26**(2): 67–71, 2000.
16. F. Huang, K. Li and A. Kulachenko A. Measurement of interfiber friction force by atomic force microscopy. In proc. *Annual Meeting 2009*, pp183–190, Montreal, Canada. PAPTAC, Montreal 2009.
17. S.R. Andersson and A. Rasmuson. Dry and wet friction of single pulp and synthetic fibres. *Journal of Pulp and Paper Science*. **23**(1):J5–J11, 1997.
18. R. Maboudian and R.T. Howe. Critical review: Adhesion in surface micromechanical structures. *Journal of Vacuum Science and Technology B*. **15**(1):1–20, 1997.
19. R.S. Seth, D.H. Page, M.C. Barbe and B.D. Jordan. The mechanism of the strength and extensibility of wet webs. *Svensk Papperstidning*. **87**(6):R36–R43, 1984.

20. R.J. Seth. The effect of fibre length and coarseness on the tensile strength of wet webs: a statistical geometry explanation. *Tappi J.* **78**(3):99–102, 1995.
21. A. Tejado and T.G.M. van de Ven. The strength of wet paper: Beyond capillary forces. In proc. *Papermaking Research Symposium*, 9p, Kuopio, Finland. University of Kuopio, Kuopio, 2009.
22. H. Nanko and J. Ohsawa. Mechanisms of fibre bond formation. In **Fundamentals of Papermaking**, Trans. 9th Fund. Res. Symp. (eds. C.F. Baker and V.W. Punton), pp783–830, Mechanical Engineering Publications Ltd., London, 1989.
23. R. Pelton. A model of the external surface of wood fibers. *Nordic Pulp and Paper Research J.* **8**(1):113–119, 1993.
24. M.A. Hubbe. Bonding between cellulosic fibers in the absence and presence of dry-strength agents – A review. *BioResources.* **1**(2):281–318, 2006.
25. P. Myllytie. Interactions of polymers with fibrillar structure of cellulose fibres: A new approach to bonding and strength in paper, Dissertation, Department of Forest Products Technology, Helsinki University of Technology, Espoo, 2009.
26. R. Pelton, J. Zhang, L. Wågberg and M. Rundlöf. The role of surface polymer compatibility in the formation of fiber/fiber bonds in paper. *Nordic Pulp and Paper Research J.* **15**(5):400–406, 2000.
27. K. Niskanen, J. Mäkinen, J. Ketoja, J. Kananen and R. Wathén, R. Paper industry invests in better web runnability. *Paperi ja Puu.* **85**(5):274–278, 2003.
28. A. Tanaka, J. Asikainen and J. Ketoja. Wet web rheology on a paper machine. In **Advances in pulp and paper research**, Trans.14th Fund. Res. Symp., (ed. S.J. I’Anson), pp577–595, Pulp and Paper Fundamental Research Society, Bury, 2009.
29. M. Ora. The effect of web structure on wet web runnability, Dissertation, Department of Forest Products Technology, Aalto University, Espoo, 2012.
30. A. J. Barnet and D.M. Harvey. Wet web characteristics and relation to wet end draws. Part II – Wet behaviour in the press section of an experimental paper machine. *Pulp and Paper Canada.* **81**(11):T306–T310, 1980.
31. J. Mäkinen. Testing of wet webs with KCL AHMA. Unpublished KCL report, 2003.
32. A-L. Erkkilä A-L. Mechanisms and measurements of the layered orientation structure of paper sheets (in Finnish), Licentiate thesis, Department of Physics, University of Jyväskylä, Jyväskylä, 1995.
33. M.H. Odell. Paper structure engineering. *Appita J.* **53**(5):371–377, 2000.
34. M.H. Odell and P. Pakarinen. Formation – influences and tuning. In proc. *28th EUCEPA Conference, Sustainable Development for the Pulp and Paper Industry*, pp152–168, Lisbon, Portugal. TECNICELPA, Lisbon, 2003.
35. B. Norman. Web forming. Ch. 6 in **Papermaking Science and Technology, Book 8, Papermaking Part 1, Stock Preparation and Wet End** (ed. H. Paulapuro), Finnish Paper Engineers’ Association/Paperi ja Puu Oy, Helsinki, 2008.
36. M. Avikainen and A-L. Erkkilä. Comparison of traditional β -radiography and storage phosphor screen formation measurement techniques. *Paperi ja Puu.* **85**(5):279–286, 2003.
37. M. Sonka, V. Hlavac and R. Boyle. Image processing analysis and machine vision. 2nd ed. Pacific Grove, CA, USA: Brooks/Cole Publishing Company, 1998.

38. A-L. Erkkilä, P. Pakarinen and M. Odell. 1999. The effect of forming mechanisms on layered fiber structure in roll and blade gap forming. In proc. *TAPPI 99 – Preparing for the Next Millennium*, pp389–400, Atlanta, GA. TAPPI Press, Atlanta, 1999.
39. P. Lipponen, A-L. Erkkilä, T. Leppänen and J. Hämäläinen. On the importance of in-plane shrinkage and through-thickness moisture gradient during drying on cockling and curling phenomena. In: **Advances in Pulp and Paper Research**, *Trans. 14th Fund. Res. Symp.*, (ed. S.J. I'Anson), pp389–436, Pulp and Paper Fundamental Research Society, Bury, 2009.
40. A-L. Erkkilä, P. Pakarinen and M. Odell. Sheet forming studies using layered orientation analysis. *Pulp and Paper Canada*. **99**(1):81–85,1998.
41. D.T. Hristopulos and T. Uesaka. Factors that control the tensile strength distribution in paper. In proc. *2003 International Paper Physics Conference*, pp5–17, Victoria, Canada. Pulp and Paper Technical Association of Canada, Montreal, 2003.
42. M.J. Korteoja. Damage and fracture in fibrous compounds: The effect of structural disorder, Dissertation, Laboratory of Computational Engineering, Helsinki University of Technology, Espoo, 1997.
43. O.W. Gregersen. On the assessment of effective paper web strength, Dissertation, Department of Chemical Engineering, Norwegian University of Science and Technology, Trondheim, 1998.
44. T. Uesaka, M. Ferahi, D. Hristopulos, N. Deng and C. Moss. Factors controlling press-room runnability of paper. In **The Science of Papermaking**, *Trans. 12th Fund. Res. Symp.*, (ed. C.F. Baker), pp1423–1440, The Pulp and Paper Fundamental Research Society, Bury, 2001.
45. R. Wathén and K. Niskanen. Strength distributions of running paper webs. *Journal of Pulp and Paper Science*. **32**(3):137–144, 2006.
46. H. Akaike. Information theory and an extension of the maximum likelihood principle. In proc. The 2nd International Symposium on Information Theory, pp267–281, Budapest, Hungary. 1973.
47. K.P. Burnham and D.R. Anderson. Model selection and multimodel inference. A practical information-theoretic approach. 2nd ed. Springer. 2002.
48. Wafo toolbox, A Matlab toolbox for analysis of random waves and loads. Centre for Mathematical Sciences, Lund University, Version 2.5, 2009.
49. A. Kulachenko and T. Uesaka. Direct simulations of fiber network deformation and failure. *Mechanics of Materials*. **51**:1–14, 2012.
50. T. Lappalainen and J. Kouko. Determination of local strains and breaking behaviour of wet paper using high-speed camera. *Nordic Pulp and Paper Research J*. **26**(3):288–296, 2011.
51. S. Borodulina, A. Kulachenko, S. Galland and M. Nygård. Stress-strain curve of paper revisited. *Nordic Pulp Paper Research J*. **27**(2):318–328, 2012.
52. E. Retulainen. The role of fibre bonding in paper properties. Dissertation, Laboratory of Paper Technology, Helsinki University of Technology, Espoo, 1997.
53. L. Wong, M.T. Kortschot and C.T.J. Dodson. Effect of formation on local strain fields and fracture of paper. *Journal of Pulp and Paper Science*. **22**(6): J213–J219, 1996.

54. P.A. Gradin, D. Graham, P. Nygård and H. Vallen. The use of acoustic emission monitoring to rank paper materials with respect to their fracture toughness. *Experimental Mechanics*. **48**(1):133–137, 2008.

APPENDIX 1

ABOUT THE COMPUTATION OF THE DISTRIBUTION MODELS

Maximum likelihood estimates and AIC values were computed with Matlab using the Wafo toolbox [48]. Because the toolbox provides maximum likelihood estimates only for the Gumbel distribution for maximum (5), not for the minimum (2), the computation was therefore performed using data multiplied by -1 and Equation (5). This made it possible to obtain the maximum likelihood estimates required.

$$G(x) = \exp \left[- \exp \left(- \frac{x - \mu}{\alpha} \right) \right] \quad (5)$$

where

$G(x)$ is the cumulative failure probability at tension x

μ is the location parameter

α is the scale parameter.

Transcription of Discussion

THE EFFECT OF MOISTURE AND STRUCTURE ON WET WEB STRENGTH AND ITS VARIATION – A PILOT SCALE APPROACH USING DRY AND REWETTED MILL MADE PAPERS

*Markku Ora*¹ and *Thaddeus Maloney*²

¹ UPM- Kymmene Corporation, Research Centre, FI- 53200 Lappeenranta,
Finland

² School of Chemical Technology, Aalto University, FI- 00076 Espoo, Finland

Tetsu Uesaka Mid Sweden University

I am very excited about the results presented in your talk. First of all, concerning the conclusions about the difference between the shape and uniformity of the distributions of dry strength and wet strength. This result exactly fits the current knowledge of the statistical failure of disordered materials. What is known is that extreme value statistics do not exactly apply to very complex systems like a fibre network and all other disordered materials. However, when the system is relatively brittle, load concentrates in local areas during failure due to failure at individual defects. In such a system, the Weibull distribution is, once again, quite a good approximation, meaning that dry strength very much follows the Weibull distribution. On the other hand, in more ductile systems where individual defects fail, force (or stress) does not concentrate in this area and the force is shared by other areas at a larger scale. In such systems the distribution is actually following the Gaussian distribution, which is exactly as shown in your results. Also, uniformity increases as we increase the sample size so that, if you used this pilot-scale tester with the wider spacing, you would see an even more uniform wet strength distribution which follows the Gaussian distribution. Therefore your

Discussion

observations and conclusions fit well with the current knowledge in this area. So, I am really impressed and also very much encouraged by the result.

Markku Ora

Thank you.

Bob Pelton McMaster University

This is very nice work. Do you think your conclusions would also hold for paper types that employ wet strength resins? I assume that they are not normally used for a coating base stock, but if you had chemical agents in there that gave you stronger fibre-fibre bonds when wet, would you see the same effects and make the same conclusions?

Markku Ora

If the chemistry has an influence on the friction between the wet fibres, it has an influence on how easily the wet fibres can slide in relation to each other. The influence of a wet strength additive depends on its effect on the bonding mechanism. Therefore I think that the wet web behaviour should be the same as shown here.

Peter de Clerck Amazon Papyrus

In paper making, for wet web strength, it is very common to use extra long fibre to improve the sustainability of the sheet with variations in draw on the production machine. There seems to be some correlation between the fibre length and the tolerable intensity of variation in the formation in the sheet. Have you done any work at all looking at the effect of fibre length in the context of acceptable formation and wet web strength?

Markku Ora

No, during this work, I did not look at this issue. If I could have used the results for the LWC base papers where the chemical pulp content was quite high, I would certainly have answers to this question but, as I mentioned, orientation and formation correlated so badly that I could not use those data. In other research, that I have been doing, I have not looked at the effect of fibre length. So, I do not have an answer to your question.